In vitro efficacy and *in vivo* toxicity and retention of targeted nanoformulated carboplatin in a sustained release carrier for treatment of osteosarcoma.

Sustained release osteosarcoma targeted nanoformulated carboplatin

Kevin Day[1], Marije Risselada[2*¶], Marina Sokolsky-Papkov[1¶]

[1] Center for Nanotechnology in Drug Delivery, Division of Pharmacoengineering and Molecular Pharmaceutics, UNC Eshelman School of Pharmacy, UNC-Chapel Hill

[2] Department of Veterinary Clinical Sciences, College of Veterinary Medicine, Purdue University, 625 Harrison Street, West Lafayette, Indiana 47907

* Corresponding author; Email: mrissela@purdue.edu

¶ These authors contributed equally

Author contributions: Day: made the particles, performed the in vitro parts of the study; Risselada: envisioned the project & study design, obtained grant funding, performed the live animal study, data analysis, maintained oversight of the project, co-wrote the manuscript; Sokolsky: envisioned the project & study design, obtained grant funding, performed the in vitro part of the study, data analysis, maintained oversight of the project, co-wrote the manuscript.

Abstract

Objective: evaluate 1) if targeting of platinum magnetic nanoclusters will promote uptake in osteosarcoma cells *in vitro*, 2) targeting will improve uptake and delivery in murine OSA *in vivo* compared to free carboplatin, 3) incorporation into a sustained release carrier (SRC) will prolong local retention *in vivo*.

Methods: Complex stability and peptide loading was assessed. Drug release was tested at pH 7.4 and 5.5 and cellular uptake and cytotoxity determined for canine, human and mouse osteosarcoma. Subcutaneous murine osteosarcoma was induced and optimal dose and time until tumor growth were established. Tumor bearing mice were equally distributed between 8 treatment (0.5mg carboplatin/mouse) and 1 control group and sacrificed at 8 predetermined time points between 1 hour and 8 days. Blood, tumor site and organs were harvested for tissue ferron and platinum content analysis (ICP-MS).

Results: Carboplatin was preferentially released at pH5.5. Targeting increased cellular uptake for carboplatin 15.2-fold, and decreased IC_{50} at 24h and 48h. At 2 weeks, a SC injection of $1\text{-}1.5^{6}$ live cells/mouse reliably resulted in a palpable tumor. Plasma platinum peaked prior to 6 hours while plasma ferron peaked at 24-48 hours. Intratumoral delivery did not lead to a sustained local presence while local delivery in a SRC after surgery did.

Conclusions: Targeting of MNC-carboplatin is possible with an increased osteosarcoma cell uptake *in vitro*. *In vivo* metastatic uptake could not be assessed due to lack of metastases, but local delivery in a SRC yielded high local, and low systemic platinum concentrations in mice.

Introduction

Localized cancer therapy has attracted considerable attention due to the ability to deliver higher local drug load, regardless of vascular status, and reduce systemic toxicity, with various delivery systems used (such as hydrogels,[Risselada-2017a, Risselada2016,Risselada 2020] polymers[Vishwarao2016] and calcium sulfate hemihydrate[Tulipan2016, Tulipan2017,Maxwell2020,Phillips2018,Risselada2015,Worth2020, Belda2021]). In addition, local drug delivery systems have been used to visualize and/or treat metastasis in a theranostic approach.[Li2012] Magnetic nanoparticles (MNPs) have long been studied as magnetic resonance (MR) imaging agents and are known for their biocompatibility and low toxicity.[Singh2014a, Singh2014b] Their presence could allow assessment of uptake in residual disease as well as distribution into metastatic lesions. The authors previously developed a simple theranostic nanoformulation based on magnetic nanoparticles stabilized by a bisphosphonate-modified poly(glutamic acid)-b-(ethylene glycol) block copolymer (MNC) and complexed with platinum drugs.[Vishwarao2016] Targeting the formulation with peptides based on cell specific surface receptors would allow selective delivery of carboplatin into cells. Two potential cell surface receptors have been identified for osteosarcoma (OSA): Insulin-like Growth Factor-1 Receptor (IGF-1R) described in both canine and human OSA[Hassan2012,Friebele2015, Schmidt2013,Rodriguez2014,Schiffman2015,Maniscalco2015], and Ephrin type-A receptor-A (EphA-2),[Posthuma2016] a recently discovered receptor in human OSA, but not described in canine OSA yet. Prior work showed that targeting EphA-2 receptors in ovarian cancer cells was possible.[Scarberry2008] Biodegradable or thermo-sensitive injectable or implantable polymers and gels can be used for sustained local delivery of drugs.[Sokolsky-Papkov2009, Mathews2009,Golovanevski2015, Risselada2016,Risselada2017a, Risselada2020,Risselada2024] Polymers based on polylactic acid-castor oil are solid to viscous liquid in RT

based on their composition, biocompatible and were shown to incorporate and release bupivacaine *in vivo*, prolonging the local analgesia to 96 hours,[Sokolsky-Papkov2009,Golovanevski2015] and release rates can be tuned further based on the polymer composition. These polymers can successfully incorporate and release nanoparticles.[Lee2017] Tissue adherent microgels based on oxidized dextran form an in situ-depot by reacting with amino groups present in the proteins in the injection site.[Denga2016] We propose to incorporate targeted MNC formulated carboplatin (t-MNC-carboplatin) into injectable polymers based on polylactic acid-castor oil and tissue adherent microgels.

The aims for this study were to: 1) evaluate if t-MNC-carboplatin can selectively promote the uptake of carboplatin into cancer cells and enhance its activity against murine OSA *in vitro*, 2) t-MNC-carboplatin will improve uptake and delivery in murine OSA *in vivo* compared to free carboplatin, 3) incorporation into a sustained release carrier (SRC) will prolong local retention *in vivo*. Our hypotheses were that 1) t-MNC-carboplatin would be stable *in vitro* with a similar IC_{50} and an increased cellular uptake compared to free carboplatin and non-targeted MNC-carboplatin, 2) targeting would increase uptake *in vivo*, and would lead to an improved outcome compared to free carboplatin while 3) incorporation into a SRC would prolong local retention.

Materials and Methods

MNCs preparation, in vitro stability, IC_{50} and cellular uptake

Particle loading and *in vitro* drug release:

85 Magnetic nanoclusters (MNCs) were prepared as previously described.[Vishwarao2016] Specifically,
86 magnetic nanoparticles (MNPs) with an average diameter of 9nm were stabilized by a
87 bisphosphonate-modified by polyglutamic acid homopolymer or poly(glutamic acid)-b-(ethylene
88 glycol), poly(aspartic acid)-b-(ethylene glycol) block copolymers. Cisplatin or carboplatin was
89 loaded as previously described and the drug loading was measured by ICP-MS.[Vishwarao2016]
90 MNCs stability with or without drug:
91 The targeting peptides based on EphA-2 (EphA-2-binding peptide, peptide 66) and IGF-1R
92 (IGF-1R-binding peptide, peptide 67) were conjugated to the polymer carboxylic side chains
93 through EDC/S-NHS chemistry and purified using filter centrifugation. The conjugation
94 efficiency and the targeting peptide content was determined by HPLC analysis of non-conjugated
95 peptide. The polylactic acid-castor oil block copolymer for the SRC was prepared as previously
96 described[Sokolsky-Papkov2009b] at 50:50 ratio of castor oil to lactic acid. The sustained release
97 formulation was prepared by directly mixing the carboplatin/t-MNC-carboplatin into the polymer
98 at 5% w/w. The particles were dispersed in PBS pH 7.4 and ABS pH 5.5 and the Pt release was
99 measured by ICP-MS as previously described.[Vishwarao2016]
100 A 14-day elution curve was obtained of 1) t-MNC-carboplatin, 2) carboplatin in SRC x 3;
101 3) t-MNC-carboplatin in SRC. The release of the drug-loaded nanoparticles was compared to the
102 release of the free drug. The load % of coated particles was measured using ICP-MS as
103 previously described.[Vishwarao2016]
104 ***In vitro* cellular uptake and cytotoxicity:**
105 Enhancement of cellular uptake by OSA cells by using the proposed targeting peptides was
106 evaluated as follows: 6-well plates were seeded with 10^6 cells each and treated for 24hrs with: 1)
107 carboplatin; 2) MNC-carboplatin and 3) t-MNC-carboplatin, after which the cells were washed,

108 harvested and lysed. Pt and Fe cellular content was measured by ICP-MS using a prior described
109 protocol.[Vishwarao2016]

110 *In vitro* cytotoxicity of the new carboplatin formulation was assessed in canine OSA:
111 OSCA-40 (cell line made available for *in vitro* use by Dr M. Hauck) and D17 (ATCC, Manassas,
112 Virginia, US) as well as human OSA (CRL-1543, ATCC) and mouse OSA (K7M2wt, ATCC)
113 for carboplatin and cisplatin. Twenty-four hours after seeding about 3000 cells/well in 96-well
114 plates, the cells were treated for 24 and 48 hrs. A colorimetric assay (Cell Titer Blue Cell
115 Viability Assay, Promega, Madison, WI, US) that detects cellular metabolic activities was used
116 to assess cell viability. The cell viability was determined by comparing the different treatment
117 groups with the control (untreated) wells. Three different treatment combinations were evaluated
118 for each cell line: 1) carboplatin; 2) MNC-carboplatin; 3) t-MNC-carboplatin; 4) cisplatin; 5)
119 MNC-cisplatin and 6) t-MNC-cisplatin.

120

121 *In vivo* murine subcutaneous osteosarcoma model

122 Institutional IACUC approval was obtained (PACUC #1711001644) for this study.
123 Osteosarcoma cells (K7M2wt, ATCC) were injected in the subcutaneous space over the dorsum
124 of fourteen female BALB/c mice of approximately 20-gram body weight (Charles River). Live
125 cells were harvested, diluted and suspended in 100uL ice-cold sterile buffered saline per dose,
126 according to prior published protocols [Overwijk2001] Three doses were evaluated for tumor growth:
127 2^5 (n=4) 5^5 (n=4) and 1^6 (n=6). Mice were monitored daily to pinpoint a day post inoculation at
128 which tumor growth reliably occurred to use for the remainder of the study.

129

In vivo outcome, local retention, distribution and efficacy

In vivo efficacy was evaluated using the optimized mouse model: 1.5^6 K7M2wt cells in 100uL were injected subcutaneously over the dorsum of 192 female BALB/c mice. Eight treatment groups were included, and three mice were sacrificed at 8 time points [1 hour, 6 hours, 12 hours, 1 day, 2 days, 3 days, 5 days, and 8 days] for each group. Treatment groups were: control (control), intraperitoneal (IP) non-targeted MNC-carboplatin with surgery to remove the primary tumor; IP non-targeted MNC-carboplatin without surgery to remove the primary tumor; IP t-MNC-carboplatin with surgery to remove the primary tumor; IP t-MNC-carboplatin without surgery to remove the primary tumor; intratumoral injection of t-MNC-carboplatin without surgery; surgical removal of the primary with local delivery of t-MNC-carboplatin in polymer; surgical removal of the primary with local delivery of non-targeted MNC-carboplatin in polymer. The total dose per mouse was 0.5mg carboplatin in a total volume of 0.1ml. The drug was filtered immediately prior to administration (20micron filter, Corning; Kentucky, USA) and aseptically handled thereafter. The formulation in a SRC was aseptically handled but not filtered immediately prior to administration. Mice were checked daily for incisional complications and overall health. After euthanasia, the wound bed and all internal organs were grossly examined. The wound bed was evaluated for necrosis, dehiscence and for residual or recurrent disease. The ventral and dorsal aspects of the lungs were photographed to allow quantification of any metastatic lesions present within the lung and the number/size of metastases were counted and measured. Samples obtained were: plasma, primary tumor/wound bed, lungs (areas macroscopically free and with macroscopic metastases were collected separately) as well as liver

151 and kidneys. All samples were weighed prior to freezing to -70ºC and were processed in one

152 batch for measurement of Pt & Fe content using ICP-MS analysis.

153 # Results

154 ## *In vitro* evaluation of stability, IC_{50} and cellular uptake

155 **Particle loading and *in vitro* drug release:**

156 Particle loading (expressed as drug load %) ranged from 5.12-9.24% (Table 1, Table 2, Fig 1)
157 with load % of the targeted formulation lower but comparable, and drug load of cisplatin higher
158 than carboplatin. All particles released fully from the polymer, with an increased drug release in
159 pH 7.4 and when coupled to a peptide (Figure 1). Drug release was increased in pH 7.4
160 compared to pH 5.5 and when coupled to a peptide. Cisplatin did not exhibit the same pH
161 triggered release post peptide conjugation while carboplatin release increased post peptide
162 conjugation (Figure 2).

163 **Table 1.** Drug load percentage (measured using ICP-MS) expressed as %

Sample	Drug load%
MNC-carboplatin	6.26
MNC-carboplatin-peptide	5.12
MNC-cisplatin	9.24
MNC-cisplatin-peptide	8.20

164 Drug loading for both targeted and non-targeted carboplatin and cisplatin is shown.
165 MNC=magnetic nanoclusters
166
167 **Table 2.** Influence of coating on drug loading (measured using ICP-MS) expressed as %.
168 Polyglutamic coated particles had a higher carboplatin load %

Sample	Fe %	Fe3O4 %	Carboplatin load %
PEG113-PLD50 (PEG-Aspartic)	13.38	18.46	9.24
PLE 100 (Glutamic acid)	26.50	36.57	7.74
PEG113-PLE100 (PEG-Glutamic)	21.40	29.53	15.19

169

170 **Figure 1: Summary of *in vitro* assessment of nanoparticles pre-targeting.** The particles size,
171 PDI, stability of the carboplatin loaded particles and the pH triggered release were assessed.
172 Polyglutamic coated particles were more stable and exhibited a greater pH release effect.

173

174 **Figure 2: Percentage drug release *in vitro*.** Release of MNC-carboplatin (A) with or without
175 coupling to a peptide (B) was compared for an environment with a pH of 7.4 and 5.5. Drug
176 release was increased in pH 7.4 compared to pH 5.5 and when coupled to a peptide. Cisplatin did
177 not exhibit the same pH triggered release post peptide conjugation while carboplatin release
178 increased post peptide conjugation.

179

180 ***In vitro* cellular uptake and cytotoxicity:**

181 Conjugating with a peptide used to target EphA-2 (peptide 66) more effectively increased
182 cellular uptake compared to conjugating with an IGF-1R-binding peptide (peptide 67) or to non-
183 conjugated PLE (Table 3, Figure 3). This effect was seen for all 4 cell lines. The % cellular
184 uptake in mouse OSA cells (K7M2wt) was higher for free cisplatin and MNC loaded cisplatin
185 compared to their respective carboplatin formulations (Figure 4). MNC loading did not influence
186 cellular uptake. While targeting of the MNC-formulation increased the cellular uptake for both
187 cisplatin and carboplatin, this increase was more pronounced for carboplatin and the cellular
188 uptake for targeted-MNC-carboplatin was the highest for all formulations assessed. The MNC
189 formulation decreased the cytoxicity, while conjugating with a peptide to create a targeted
190 formulation increased the cytotoxicity (Table 4). Ultimately carboplatin conjugated with EphA-2
191 as targeting peptide was chosen for the *in vivo* part of the study due to better uptake in the cells
192 and a higher differential between targeted versus non-targeted formulations.

193

194 **Table 3.** Drug load percentage of non-targeted and targeted coated particles (measured using
195 ICP-MS) is expressed as %).

Sample	Carboplatin load %,

PLE carboplatin	1.36
PLE 66 (EphA-2 targeted) carboplatin	2.98
PLE 67 (IGF-1R targeted) carboplatin	2.66

196

197 **Table 4.** IC_{50} (after 24h hours incubation) determination of non-targeted clusters: no significant
198 differences between formulations. Polyglutamic coated particles performed better than
199 polysaspartic coated particles. HOS: Human osteosarcoma, K7M2wt: murine osteosarcoma, D17
200 and OSCA: canine osteosarcoma.

Cell type	Drug and Coating	IC_{50} ug/ml
HOS	**Carboplatin**	**22.09**
	Polyglutamic-PEG (PLE-PEG)	29.15
	Polyglutamic acid (PLE)	28.31
	Polyaspartic acid-PEG (PLD-PEG)	28.28
K7M2wt	**Carboplatin**	**18.39**
	Polyglutamic-PEG (PLE-PEG)	26.98
	Polyglutamic acid (PLE)	15.35
	Polyaspartic acid-PEG (PLD-PEG)	24.38
D17	**Carboplatin**	**119.89**
	Polyglutamic-PEG (PLE-PEG)	99.83
	Polyglutamic acid (PLE)	103.77
	Polyaspartic acid-PEG (PLD-PEG)	142.93
OSCA	**Carboplatin**	**117.59**
	Polyglutamic-PEG (PLE-PEG)	80.39
	Polyglutamic acid (PLE)	81.98
	Polyaspartic acid-PEG (PLD-PEG)	83.17

201
202

203 **Figure 3: Assessment of two targeting peptides.** A, B uptake of Ferron and Platinum in 4
204 osteosarcoma cell lines. C: uptake in murine osteosarcoma, D: Structure of peptide 66.
205 Peptide 66 was targeted at binding to EphA-2, peptide 67 targeted at IGF-1R. Conjugating with
206 EphA-2-binding peptide resulted in increased cellular uptake for murine (K7M2wt), human
207 (HOS) and canine (OSCA) osteosarcoma cells *in vitro* and was chosen as the targeting peptide
208 for the remainder of the study.

209

210 **Figure 4. Cellular uptake of platinum in K7M2wt *in vitro*.** Platinum uptake in cells for
211 carboplatin and cisplatin in an (EphA-2-) targeted and non-targeted MNC formulation compared
212 to non-altered formulation. Targeting improved cellular uptake, both in cisplatin and carboplatin.

In vivo murine osteosarcoma model

None of the mice inoculated with 2^5 or 5^5 cells grew macroscopically visible or palpable tumors at the injection site. Three out of 6 mice inoculated with 1^6 cells showed palpable tumor growth at 2 weeks. An inoculation dose of $1\text{-}1.5^6$ live cells/mouse was chosen for the remainder of the study.

In vivo outcome, local retention, distribution and efficacy

All 192 mice were inoculated with $1\text{-}1.5^6$ live K7M2wt cells, and tumors allowed to grow for a minimum of 2 weeks prior to treatment at d=0. Total dose per mouse was 0.5mg of carboplatin, or 0.1ml of product. Tumors reliably grew in 128 mice and two mice per time point [1-hour, 6-hour, 12-hour, 1-day, 2-day, 3-day, 5-day, and 8-day groups] were included for all 8 treatment groups.

Outcome

Two mice died: one 6-hour mouse [IP t-MNC-carboplatin with surgery] and one 3-day mouse [IP t-MNC-carboplatin w surgery]). Two sites dehisced: the same 3-day mouse [IP t-MNC-carboplatin with surgery] that died and one 1-day mouse [IP non targeted MNC-carboplatin with surgery]. No other incisional or systemic complications were noted.

Local retention

No increased local concentration of Pt was found in the control mice, after IP injection of non-targeted MNC carboplatin with or without surgery and after IP injection of targeted MNC

235 carboplatin with or without surgery (Figure 5). High levels of both Pt and Fe were found in the
236 site after intratumoral injection for 12 hours. Local delivery of MNC-carboplatin in a SRC after
237 surgery led to an increase of both Pt and Fe measured at the site with a peak at 120 hours. The
238 non-targeted MNC-carboplatin delivered locally had elevated Pt in the site initially, but with an
239 immediate drop and without a steady increase over time. Platinum and Fe for the local sustained
240 release and intratumoral delivery groups mirrored each other over time (Figure 5).
241
242 **Figure 5. Tumor and surgery site Pt content for all groups (A), Fe content for all groups**
243 **(B), Pt and Fe content for locally delivered drugs (C).** Intratumoral delivery did not lead to a
244 sustained local presence while local delivery after surgery in a sustained release carrier (SRC;
245 polylactic acid-castor oil block copolymer) did.
246

247 Distribution

248 Plasma Pt levels for all treated mice were highest within the first 12 hours, with a peak prior to 6
249 hours and decreased thereafter. Plasma Fe levels showed a later peak at 48 hours with one outlier
250 at 24 hours (Figure 6). No increased Pt was noted in the control group mice in either liver or
251 renal tissue assessed (Figure 7). All mice with IP delivered non-targeted MNC-carboplatin
252 showed high Pt content in renal tissue, whereas the Fe concentration in renal tissue was lower
253 than in lung, and especially liver. There was no high uptake in the surgery site or in non-removed
254 tumors, although uptake seemed slightly higher in sites that had tumors removed versus those
255 that did not. Intraperitoneal t-MNC-carboplatin similarly had high renal Pt content than in liver
256 or lung, but lower Fe renal content, although the effect for Pt was less pronounced. These
257 increases were not seen for locally delivered carboplatin.

258

259 **Figure 6. Plasma Platinum (Pt) and Ferron (Fe) are shown for the entire study duration,**
260 **and for the first 48hours.** A: Plasma Pt and Fe over 192 hours, B: Plasma Pt and Fe for the first
261 48 hours, C: Plasma Pt only over 192 hours; D: Plasma Fe only over 196 hours. Plasma Pt
262 peaked earlier than plasma Fe: Plasma Pt peaked prior to 6 hours whereas plasma Fe peaked at
263 24-48 hours.

264

265 **Figure 7. Platinum (Pt) and Ferron (Fe) for implantation site, lung, liver and kidney at**
266 **time point are shown for the control and 7 treatment groups.** For each variable the solid
267 symbol represents Pt, and the corresponding nonsolid symbol/color represents Fe. The left Y-
268 axis shows Pt and the right Y-axis Fe concentration. Locally delivered carboplatin consistently
269 had higher local concentrations with less systemic uptake, whereas IP delivered carboplatin had
270 higher systemic uptake.

271

272 Efficacy

273 No macroscopically visible lung metastases were seen in any of the mice. Intraabdominal lesions
274 were seen in 2 mice (one 5-day mouse with disseminated lesions [IP MNC-carboplatin without
275 surgery] and one 6-hour mouse in which the primary tumor grew into the abdomen [control
276 group].

Discussion

In the *in vitro* portion of this study, polyglutamic coated particles were found to be more stable and exhibited a greater pH release effect than other formulations. Targeting of both nanoformulated carboplatin and cisplatin with either an EphA-2-binding peptide or IGF-1R-binding peptide was possible, and the formulations yielded a similar platinum load as the non-targeted formulations. Targeting increased cellular uptake of the formulation *in vitro* in osteosarcoma cells in across species, with use of an EphA-2-binding peptide providing a more consistent and reliable increase in uptake than non-targeted or use of an IFG-1R-binding peptide. The % uptake by targeting the formulation was more pronounced for carboplatin than for cisplatin. Polyglutamic coated particles & carboplatin targeted with an EphA-2-binding peptide were chosen for the *in vivo* part of the study. A local tumor model with K7M2wt was successfully reproduced in mice but did not create distant metastases. Intratumoral delivery reached high local concentrations initially, but rapidly declined thereafter, without systemic uptake in mice. Local delivery in a sustained release compound yielded high local, and low systemic Pt concentrations. Platinum retention and distribution did not fully mirror Ferron distribution.

Two cell surface receptors were chosen as possible targets to investigate in this study. These were IFG-1R (described in both human and canine osteosarcoma)[Hassan2012,Friebele2015, Schmidt2013,Rodriguez2014,Schiffman2015,Maniscalco2015] and EphA-2 (described in human but not in canine osteosarcoma).[Posthuma2016] Neither receptor has been described in mouse osteosarcoma. The presence of EphA-2 has been associated with malignancy in various human cancers.[Wykosky2005,

299 [Xiao2020] The synthetic peptide analogues for both cell surface receptors were successfully
300 incorporated into the targeted formulations investigated in this study, with a platinum load % that
301 was similar, but smaller compared to the non-targeted formulations (5.1% vs 6.3% for
302 carboplatin and 8.2 vs 9.2% for cisplatin).
303
304 While the MNC formulation in itself had decreased cellular uptake, targeting of the formulation
305 subsequently increased uptake in OSA cells *in vitro* across species. Targeting based on an
306 EphA-2-surface receptor outperformed targeting based on IFG-1R *in vitro*. While cisplatin had a
307 higher platinum load %, the pH triggered release and increased cellular uptake of carboplatin
308 was why ultimately carboplatin was chosen for the *in vivo* portion of the study. We further chose
309 to include various treatment groups while focusing on one binding peptide (based on an EphA-2-
310 binding peptide).
311
312 A subcutaneous osteosarcoma tumor model was recreated using an adaptation of protocols that
313 utilized an injection into an appendicular bone (femur [Miretti2008] or proximal tibia [Cole2011,Crasto2018]).
314 Two mice had a local wound dehiscence, however, this most likely could be attributed to
315 residual tumor in the surgery site rather than secondary to local drug delivery as both mice
316 received carboplatin IP and not locally. The overall lack of local tissue and wound complications
317 was in line with prior studies where carboplatin was administered subcutaneously with a
318 different SRC, either in poloxamer[Risselada2017a] or in $CaSO_4$ beads.[Belda2021] However, due to
319 differences in species (rats[Risselada2017a, Belda2021] vs mice) and methodology (local Pt only measured
320 at d7[Risselada2017a], d28 [Belda2021] vs multiple time points up to d7), no direct comparison of the SRC's
321 ability to local retain carboplatin could be made.

Intratumoral delivery reached high local concentrations initially, but rapidly declined thereafter, without systemic uptake. Local delivery of both targeted and non-targeted MNC-carboplatin in a sustained release compound (polylactic acid-castor oil block copolymer) did yield high local, and low systemic Pt concentrations in mice. This is similar to other local delivery methods.[Belda2021, Risselada2017a]

Targeting of the formulation did not result in peripheral tumor uptake when delivered intraperitoneally, which could be due to the amount of drug taken up in circulation and therefore reaching the tumor site. Local delivery, however, might lead to accumulation in draining (sentinel) lymph nodes via lymphatic drainage, rather than relying on systemic circulation. This effect could be increased if the drug is selectively taken up in osteosarcoma cells due to targeting of the formulation. Further studies utilizing local drug delivery in an area with clear established locoregional draining lymph nodes in a larger sized species might be needed to fully investigate this potential. Platinum retention and distribution did not fully mirror Ferron in the current study. The ability to use the formulation to serve as a theranostic drug and have diagnostic purposes in addition to therapeutic effects, both should have a similar pattern. Follow up studies are therefore needed to fully investigate if Fe uptake in local lymph nodes or metastatic lesions or does mirror each other and therefore would provide the diagnostic arm of the formulation.

343 # Limitations

344 Several limitations to the study exist, firstly only low numbers per group were included, and had
345 variation between the values obtained. This precluded making a full pharmacokinetic analysis,
346 and results are therefore more descriptive and observational, and should be seen as pilot data. We
347 purposefully opted to increase the number of variations rather than numbers per group in this
348 pilot project to gather data for future larger studies. Despite the low numbers some conclusions
349 regarding local retention and absence of local toxicity could be drawn. A second limitation was
350 the lack of visible metastases, disallowing the assessment of uptake in metastatic lesions.
351 Development of pulmonary metastases in a mouse osteosarcoma model has been described prior,
352 both with the same cell line[Crasto2018], and with different tumor cell lines.Cole2011,[Miretti2008] It is
353 possible that the chosen injection site in our study (subcutaneous) does not lend itself well to
354 cancer spread compared to an intrafemoral [Miretti2008] or proximal tibial[Cole2011,Crasto2018] injection
355 site. We chose the subcutaneous site, as tumor growth needed to be readily visible, and tumor
356 removal feasible with a minor surgery.
357 A third limitation was due to the maximum volume that could be delivered locally or
358 intratumorally. This limited the dose that could be delivered, including for IP delivery, as the
359 dose was kept consistent between mice.
360

361 # Conclusions

362 Targeting of MNC-carboplatin was possible with use of EphA-2-binding peptide resulting in an
363 increased osteosarcoma cell uptake *in vitro* for various species. *In vivo* metastatic uptake in mice
364 and efficacy could not be assessed due to lack of metastases, but local delivery in a SRC yielded
365 high local, and low systemic Pt concentrations.

366 # References

367 Belda B, Ramos-Vara J, Messenger KM, et al. Pharmacokinetic and safety assessment of
368 carboplatin-impregnated calcium sulfate hemihydrate beads in eight rats. Vet Surg
369 2021;50(8):1650-1661.

370 Bergman NS, Urie BK, Pardo AD, et al. Evaluation of local toxic effects and outcomes for dogs
371 undergoing marginal tumor excision with intralesional cisplatin-impregnated bead placement
372 for treatment of soft tissue sarcomas: 62 cases (2009-2012). J Am Vet Med Assoc
373 2016;248:1148-1156.

374 Cole HA, Ichikawa J, Colvin DC, et al. Quantifying intra-osseous growth of osteosarcoma in a
375 murine model with radiographic analysis. J Orthop Res. 2011; 29:1957–62

376 Crasto JA, Fourman MS, Morales-Restrepo A, et al. Disulfiram reduces metastatic osteosarcoma
377 tumor burden in an immunocompetent Balb/c orthotopic mouse model. Oncotarget, 2018; 9
378 (53):30163-30172.

379 Denga Y, Yanga F, et al. Improved i.p. drug delivery with bioadhesive nanoparticles. PNAS
380 October 11, 2016; 113 (41):11453-11458.

381 Dorbandt DM, Lundberg AP, Roady PJ, et al. Surgical excision of a feline orbital lacrimal gland
382 adenocarcinoma with adjunctive cryotherapy and carboplatin-impregnated bead implantation.
383 Vet Ophthalmol 2018;21:419-425.

384 Friebele JC, Peck J, et al. Osteosarcoma: A meta-analysis and review of the literature. Am J
385 Orthop (Belle Mead NJ) 2015;44(12):547-53.

386 Golovanevski L, Sokolsky-Papkov, et al. In vivo study of an extended release bupivacaine
387 formulation following site-directed nerve injection. Journal of Bioactive and Compatible
388 Polymers 2015; 30 (1): 114-125.
389 Hassan SE, Bekarev M, et al. Cell surface receptor expression patterns in osteosarcoma. Cancer
390 2012; 118(3):740-9.
391 Hess TA, Drinkhouse ME, Prey JD, et al. Analysis of platinum content in biodegradable
392 carboplatin-impregnated beads and retrospective assessment of tolerability for intralesional
393 use of the beads in dogs following excision of subcutaneous sarcomas: 29 cases (2011-2014).
394 J Am Vet Med Assoc 2018;252:448-456.
395 Hottmann NM, Raines K, Droog M, et al. In vitro elution of amikacin from four hydrogel
396 preparations: A pilot study. Vet Surg 2023;52(3):460-466. doi: 10.1111/vsu.13914.
397 Kuntz CA, Dernell WS, Powers BE, et al. Prognostic factors for surgical treatment of soft-tissue
398 sarcomas in dogs: 75 cases (1986-1996). J Am Vet Med Assoc 1997;211:1147-1151.
399 Lee PW, Shukla S, et al. Biodegradable Viral Nanoparticle/Polymer Implants Prepared via Melt-
400 Processing. ACS Nano, ACS Nano 2017; 11: 8777−8789.
401 Li S, Goins B, et al. Feasibility of eradication of breast cancer cells remaining in
402 postlumpectomy cavity and draining lymph nodes following intracavitary injection of
403 radioactive immunoliposomes. Mol Pharm. 2012; 4;9(9): 2513-22.
404 Maniscalco L, Iussich S, et al. Increased expression of insulin-like growth factor-1 receptor is
405 correlated with worse survival in canine appendicular osteosarcoma. Vet J. 2015; 205(2): 272-
406 80.

407 Marconato L, Comastri S, Lorenzo MR, et al. Postsurgical intra-incisional 5-fluorouracil in dogs
408 with incompletely resected, extremity malignant spindle cell tumours: a pilot study. Vet
409 Comp Oncol 2007;5:239-249.
410 Mathews KG, Linder KE, Davidson GS, et al. Assessment of clotrimazole gels for in vitro
411 stability and in vivo retention in the frontal sinus of dogs. Am J Vet Res 2009; 70: 640–647.
412 Maxwell EA, Phillips H, Clark-Price SC, et al. Pharmacokinetics of platinum and safety
413 evaluation of carboplatin-impregnated calcium sulfate hemihydrate beads after implantation
414 in healthy cats. Vet Surg 2020;49:748-757
415 Miretti S, Roato I, Taulli R, et al. A mouse mode of pulmonary metastasis from spontaneous
416 osteosarcoma monitored in vivo by Luciferase imaging. PLoS ONE 3(3): e1828.
417 doi:10.1371/journal.pone.0001828
418 Morrison JG, White P, McDougall S, et al. Validation of a highly sensitive ICP-MS method for
419 the determination of platinum in biofluids: Application to clinical pharmacokinetic studies
420 with oxaliplatin. J Pharm Biomed Anal 2000;24(1):1-10.
421 Nawroth I, Alsner J, et al. Peritoneal macrophages mediated delivery of chitosan/siRNA
422 nanoparticle to the lesion site in a murine radiation-induced fibrosis model. Acta Oncol. 2013;
423 52(8):1730-8.
424 Oguri S, Sakakibara T, Mase H, et al. Clinical pharmacokinetics of carboplatin. J Clin Pharmacol
425 1988;28(3):208-15.
426 Overwijk WW1, Restifo NP. 2001 B16 as a mouse model for human melanoma. Curr Protoc
427 Immunol. 2001 May; Chapter 20: Unit 20.1. doi: 10.1002/0471142735.im2001s39.

428 Phillips H, Maxwell EA, Schaeffer DJ, et al. Simulation of spatial diffusion of platinum from
429 carboplatin-impregnated calcium sulfate hemihydrate beads by use of an agarose gelatin
430 tissue phantom. Am J Vet Res 2018;79(6):592-599. doi: 10.2460/ajvr.79.6.592.
431 Posthuma deboer J, Piersma SR, et al. Surface proteomic analysis of osteosarcoma identifies
432 EPHA2 as receptor for targeted drug delivery. Br J Cancer. 2013; 109(8): 15.
433 Risselada M, Marcellin-Little DJ, Messenger KM, et al. Assessment of in vitro release of
434 carboplatin from six carrier media. Am J Vet Res 2016;77:1381-1386.
435 Risselada M, Linder KE, Griffith E, et al. Pharmacokinetics and toxicity of subcutaneous
436 administration of carboplatin in Poloxamer 407 in a rodent model. PloS one
437 2017a;12:e0186018.
438 Risselada M, Messenger KM. Evaluation of two methods for maintaining subcutaneous
439 microdialysis after anesthetic recovery in rats. PeerJ Preprints 2017b;5:e3324v1.
440 Risselada M, Tuohy JL, Law M, et al. Local administration of carboplatin in poloxamer 407 after
441 an ulnar osteosarcoma removal in a dog. J Am Anim Hosp Assoc 2020;56(6):325-330.
442 Risselada M, Spies KE, Kim SY. Amikacin in 30% poloxamer 407 is a versatile local therapy
443 with method of application, outcome and lack of adverse effects documented in 29 dogs. J
444 Am Vet Med Assoc. 2024. Under review.
445 Rodriguez CO,Jr. Using canine osteosarcoma as a model to assess efficacy of novel therapies:
446 Can old dogs teach us new tricks? Adv Exp Med Biol. 2014; 804: 237-56.
447 Ruttalaa HB, Ramasamy T, et al. Layer-by-layer assembly of hierarchical nanoarchitectures to
448 enhance the systemic performance of nanoparticle albumin-bound paclitaxel. International
449 Journal of Pharmaceutics 2017; 519: 11–21.

450 Samuel S, Mathew BS, Veeraghavan B et al. In vitro study of elution kinetics and bio-activity of
451 meropenem-loaded acrylic bone cement. J Orthopaed Traumatol 2012; 13:131-136.
452 Singh D, McMillan JM, Kabanov AV, Sokolsky-Papkov M, et al. Bench-to-bedside translation
453 of magnetic nanoparticles. Nanomedicine (Lond). Author manuscript; available in PMC 2015
454 Feb 1. Published in final edited form as: Nanomedicine (Lond). 2014a Apr; 9(4): 501–516.
455 Singh D, McMillan JM, Liu X, Vishwasrao HM, et al. Formulation design facilitates magnetic
456 nanoparticle delivery to diseased cells and tissues. Nanomedicine (Lond). 2014b
457 Mar;9(3):469-85. doi: 10.2217/nnm.14.4. Epub 2014 Mar 19.
458 Scarberry KE, Dickerson EB, et al. Magnetic nanoparticle-peptide conjugates for in vitro and in
459 vivo targeting and extraction of cancer cells. J Am Chem Soc. 2008; 130(31): 10258-62.
460 Schiffman JD, Breen M. Comparative oncology: What dogs and other species can teach us about
461 humans with cancer. Philos Trans R Soc Lond B Biol Sci. 2015 ; 370(1673).
462 Schmidt AF, Nielen M, et al. Prognostic factors of early metastasis and mortality in dogs with
463 appendicular osteosarcoma after receiving surgery: An individual patient data meta-analysis.
464 Prev Vet Med. 2013; 112(3-4):414-22.
465 Straw RC, Withrow SJ, Douple EB, et al. Effects of cis-diamminedichloroplatinum II released
466 from D,L-polylactic acid implanted adjacent to cortical allografts in dogs. J Orthop Res
467 1994;12:871-877.
468 Sokolsky-Papkov, M, Domb AJ, et al. Impact of Aldehyde Content on Amphotericin B−Dextran
469 Imine Conjugate Toxicity. Biomacromolecules 2006; 7 (5): 1529-1535.
470 Sokolsky-Papkov, M, Golovanevski L, et al. Poly (DL: lactic acid-castor oil) 3: 7-bupivacaine
471 formulation: Reducing burst effect prolongs efficacy in vivo. Journal of pharmaceutical
472 sciences 2009a; 99 (6): 2732-2738.

473 Sokolsky-Papkov, M, Golovanevski L, et al. Prolonged local anesthetic action through slow
474 release from poly (lactic acid co castor oil). Pharm Res 2009b Jan;26(1):32-9. doi:
475 10.1007/s11095-008-9699-8. Epub 2008 Aug 22.
476 Traverson M, Stewart CE, Papich MG. Evaluation of bioabsorbable calcium sulfate hemihydrate
477 beads for local delivery of carboplatin. PLoS One. 2020;Nov 5:15(11):e0241718. doi:
478 10.1371/journal.pone.0241718.
479 Tulipan RJ, Phillips H, Garrett LD, et al. Elution of platinum from carboplatin-impregnated
480 calcium sulfate hemihydrate beads in vitro. Am J Vet Res 2016;77:1252-1257.
481 Tulipan RJ, Phillips H, Garrett LD, et al. Characterization of long-term elution of platinum from
482 carboplatin-impregnated calcium sulfate hemihydrate beads in vitro by two distinct sample
483 collection methods. Am J Vet Res 2017;78: 618-623.
484 Vishwarao HM, Master AM et al. LHRH-Targeted Cisplatin-Loaded Magnetite Nanoclusters for
485 Simultaneous MR Imaging and Chemotherapy of Ovarian Cancer. Chem. Mater. 2016; 28(9):
486 3024-3040.
487 Withrow SJ, Powers BE, et al. Comparative aspects of osteosarcoma. dog versus man. Clin
488 Orthop Relat Res. 1991; 270(270):159-68.
489 Withrow SJ, Liptak JM, Straw RC, et al. Biodegradable cisplatin polymer in limb-sparing
490 surgery for canine osteosarcoma. Ann Surg Oncol 2004;11:705-713.
491 Worth DB, Risselada M, Cooper BR, et al. Repeatability of in vitro carboplatin elution from
492 carboplatin-impregnated calcium sulfate hemihydrate beads made in a clinic setting. Vet Surg
493 2020;49:1609-1617.

494 Wu H, Cabral H, et al. Polymeric micelles loaded with platinum anticancer drugs target
495 preangiogenic micrometastatic niches associated with inflammation. J Control Release. 2014
496 Sep 10;189:1-10.13.
497 Wykosky J, Debinski W. The EphA2 receptor and ephrinA1 ligand in solid tumors: function and
498 therapeutic targeting. Mol Cancer Res. 2008;6(12):1795–806.
499 Xiao T, Xiao Y, Wang W, Tang YY, Xiao Z, Su M. Targeting EphA2 in cancer. J Hematol
500 Oncol. 2020 Aug 18;13(1):114. doi: 10.1186/s13045-020-00944-9.
501 Zamboni WC, Gervais AC, Egorin MJ, et al. Inter- and intratumoral disposition of platinum in
502 solid tumors after administration of cisplatin. Clin Cancer Res 2002;8(9):2992-2999.

Figure 1: Summary of in vitro assessment of nanoparticles pre-targeting. The particles size, PDI, stability of the carboplatin loaded particles and the pH triggered release were assessed. Polyglutamic coated particles were more stable and exhibited a greater pH release effect.

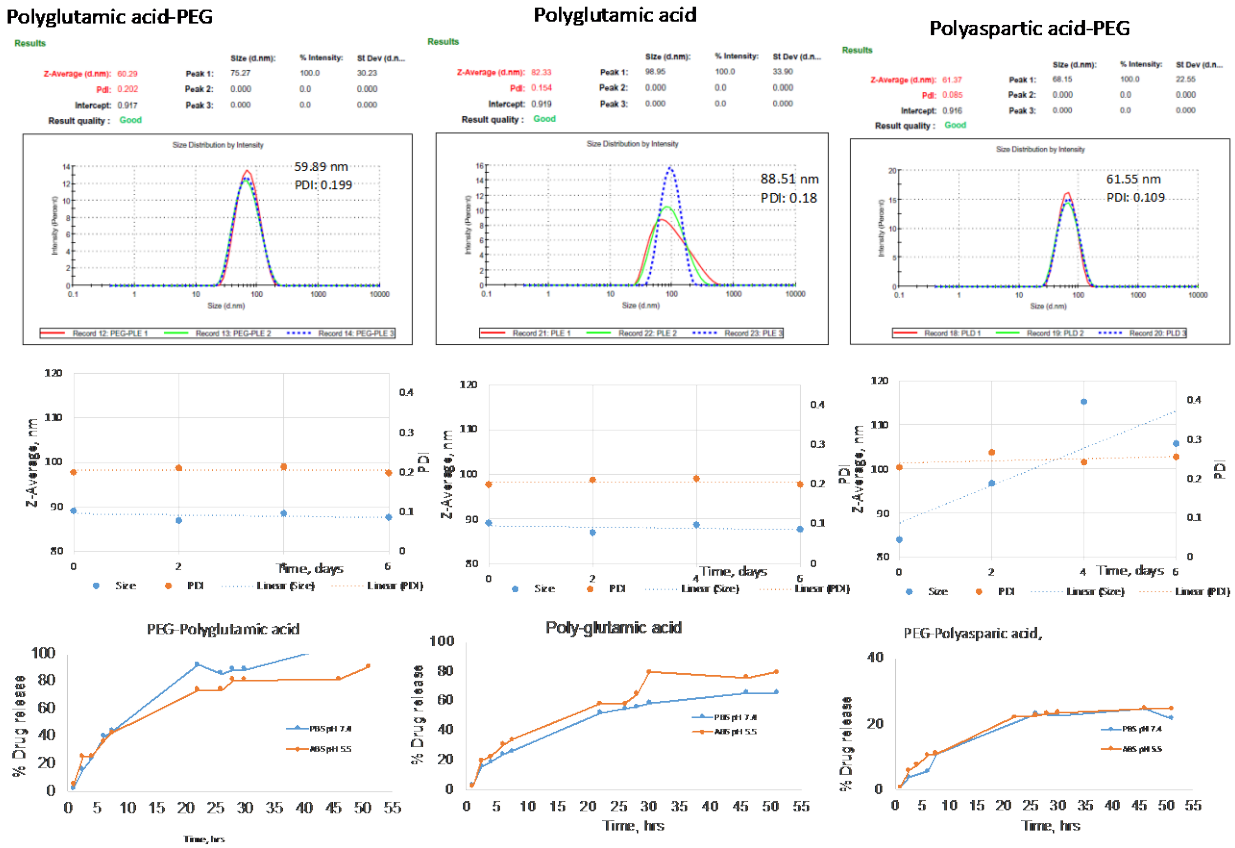

Figure 2: Percentage drug release *in vitro*. Release of MNC-carboplatin (A) with or without coupling to a peptide (B) was compared for an environment with a pH of 7.4 and 5.5. Drug release was increased in pH 7.4 compared to pH 5.5 and when coupled to a peptide. Cisplatin did not exhibit the same pH triggered release post peptide conjugation while carboplatin release increased post peptide conjugation.

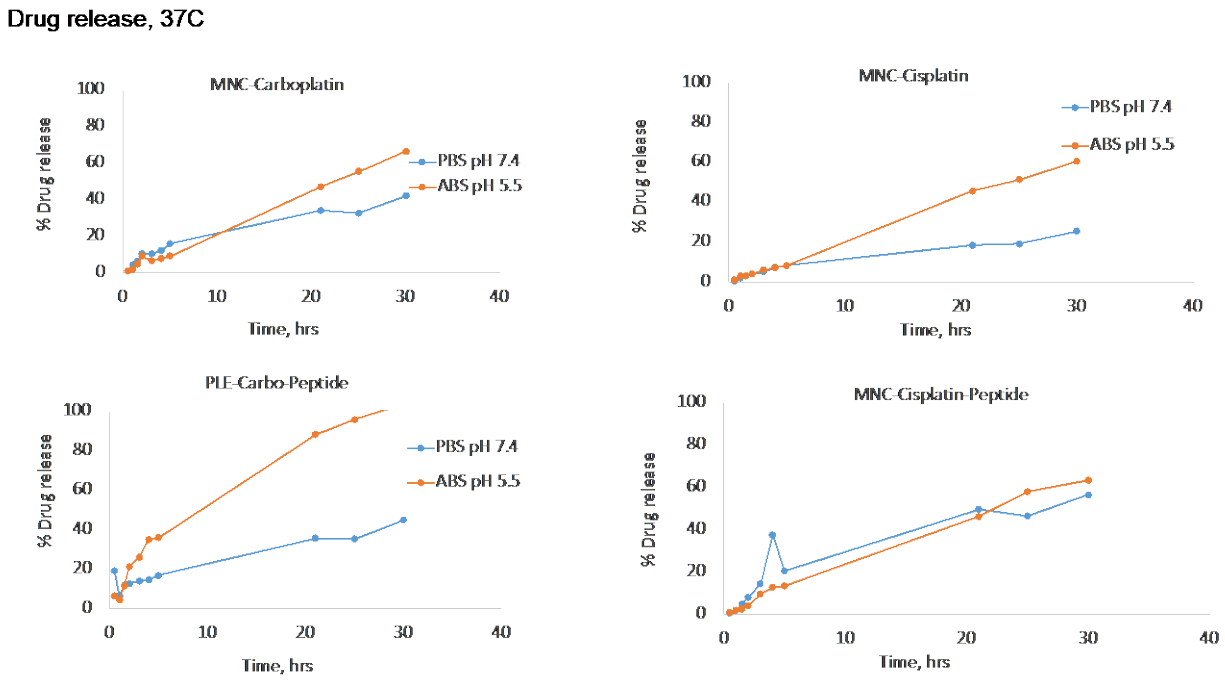

Figure 3: Assessment of two different targeting peptides. A, B uptake of Ferron and Platinum in 4 osteosarcoma cell lines. C: uptake in murine osteosarcoma, D: Structure of peptide 66. Peptide 66 was targeted at binding to EphA-2, peptide 67 targeted at IGF-1R. Conjugating with EphA-2-binding peptide resulted in increased cellular uptake for murine (K7M2wt), human (HOS) and canine (OSCA) osteosarcoma cells in vitro and was chosen as the targeting peptide for the remainder of the study.

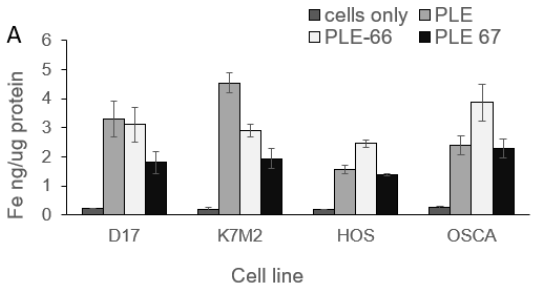

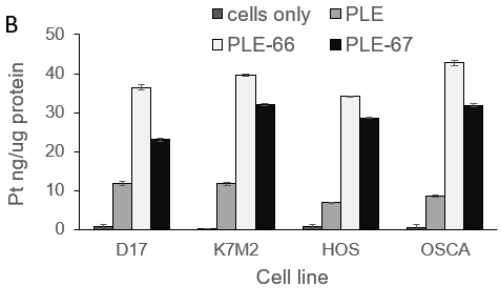

C

Polymer	Cell Type	Fe 57 ng/ug protein
PLE	K7M2	27.573
PLE-66	K7M2	37.617
PLE-67	K7M2	42.369

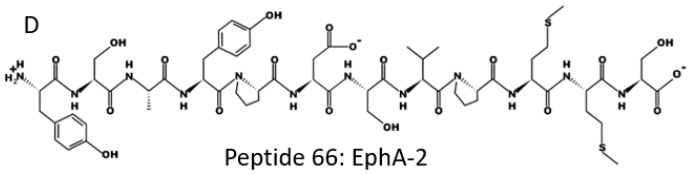

Figure 4: **Cellular uptake of platinum in K7M2wt *in vitro***. Platinum uptake in cells for carboplatin and cisplatin in an (EphA-2-)targeted and non-targeted MNC formulation compared to non-altered formulation. Targeting improved cellular uptake of carboplatin in a greater effect than cisplatin.

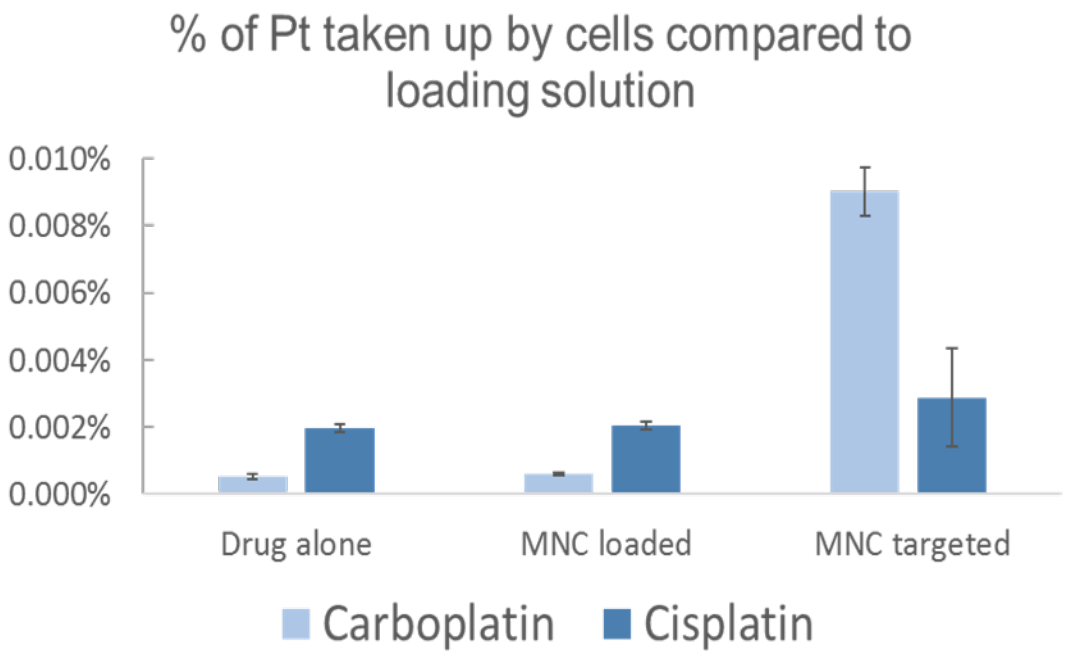

Figure 5: Tumor and surgery site Pt content for all groups (A), Fe content for all groups (B), Pt and Fe content for locally delivered drugs (C). Intratumoral delivery did not lead to a sustained local presence while local delivery after surgery in a sustained release carrier (SRC; polylactic acid-castor oil block copolymer) did.

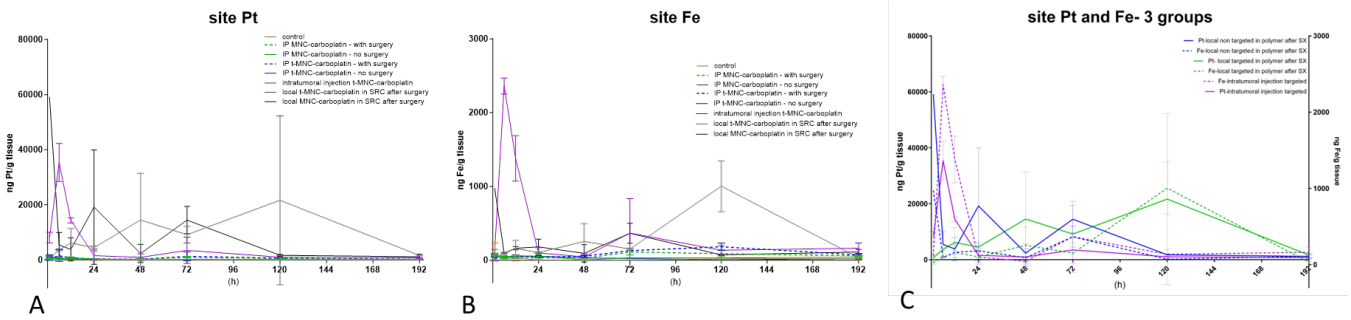

Figure 6: Plasma Platinum (Pt) and Iron (Fe) for the entire study duration, and for the first 48 hours. A: Plasma Pt and Fe over 192 hours, B: Plasma Pt and Fe for the first 48 hours, C: Plasma Pt only over 192 hours; D: Plasma Fe only over 196 hours. Plasma Pt peaked earlier than plasma Fe: Plasma Pt peaked prior to 6 hours whereas plasma Fe peaked at 24-48 hours.

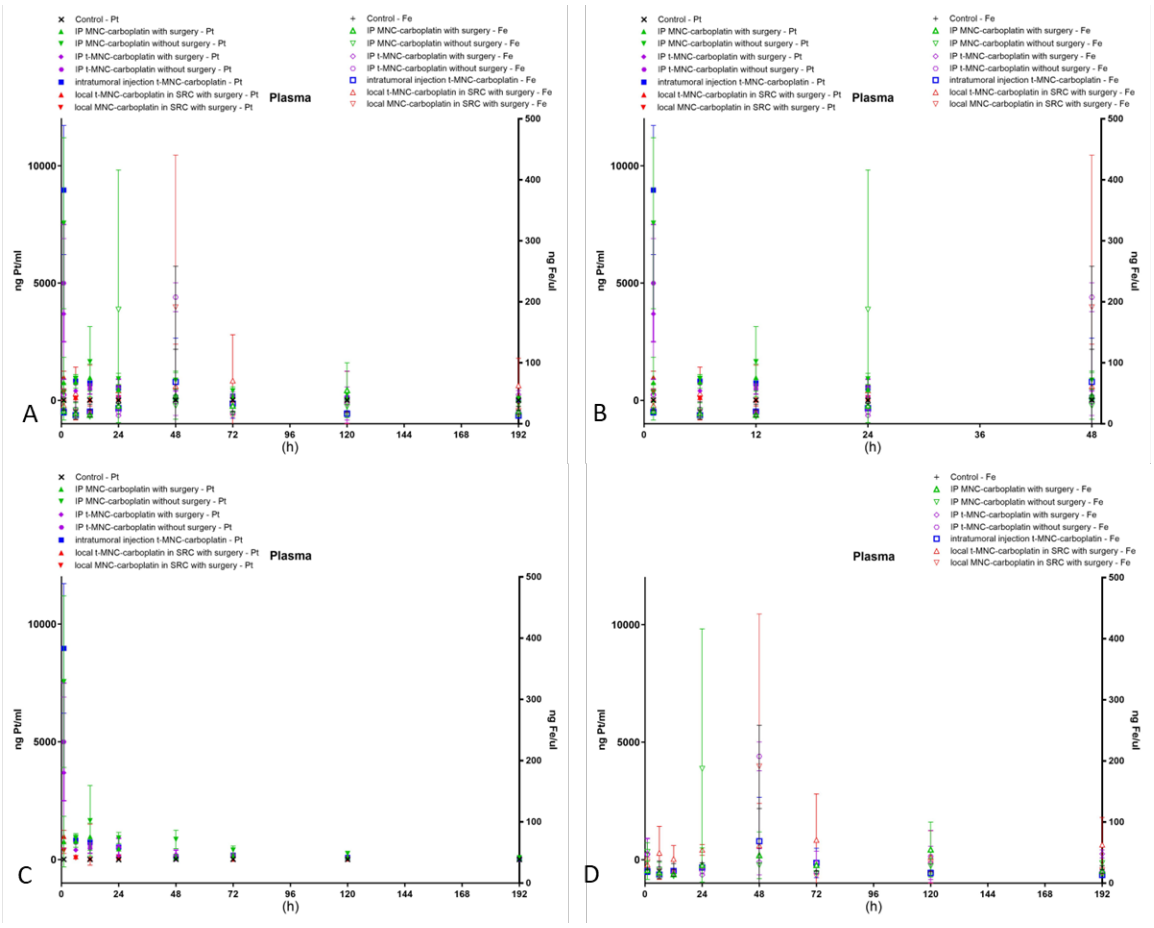

Figure 7: Platinum (Pt) and Iron (Fe) for implantation site, lung, liver and kidney at time point are shown for the control and 7 treatment groups. For each variable the solid symbol represents Pt, and the corresponding nonsolid symbol/color represents Fe. The left Y-axis shows Pt and the right Y-axis Fe concentration. Locally delivered carboplatin consistently had higher local concentrations with less systemic uptake, whereas IP delivered carboplatin had higher systemic uptake.

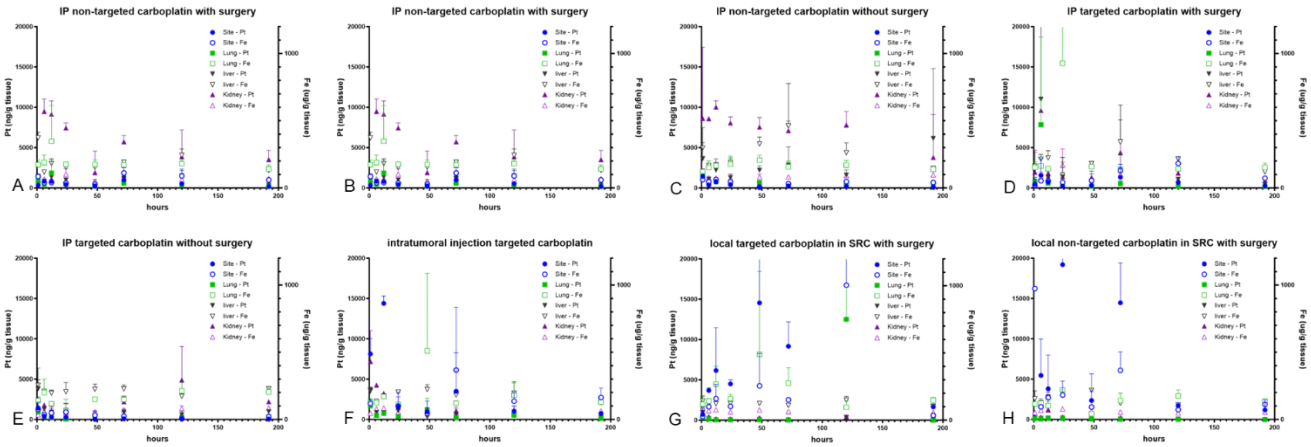

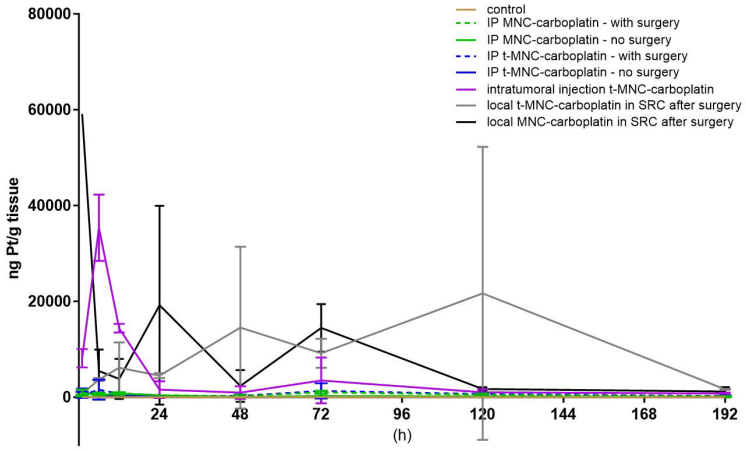
site Pt
control
IP MNC-carboplatin - with surgery
IP MNC-carboplatin - no surgery
IP t-MNC-carboplatin - with surgery
IP t-MNC-carboplatin - no surgery
intratumoral injection t-MNC-carboplatin
local t-MNC-carboplatin in SRC after surgery
local MNC-carboplatin in SRC after surgery
ng Pt/g tissue
80000
60000
40000
20000
0
24
48
72
96
120
144
168
192
(h)

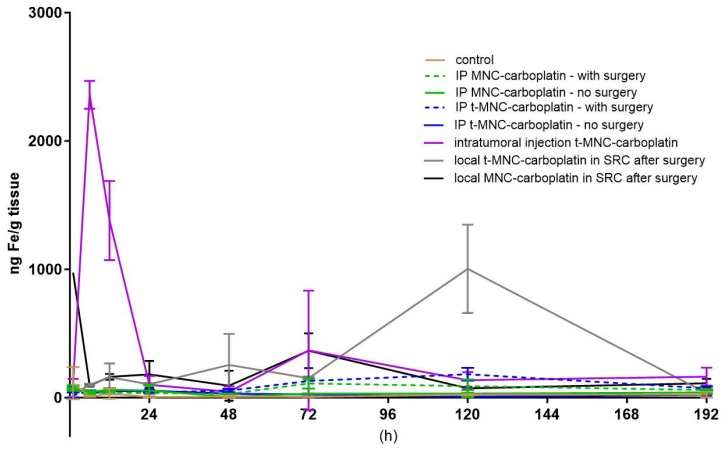
site Fe
control
IP MNC-carboplatin - with surgery
IP MNC-carboplatin - no surgery
IP t-MNC-carboplatin - with surgery
IP t-MNC-carboplatin - no surgery
intratumoral injection t-MNC-carboplatin
local t-MNC-carboplatin in SRC after surgery
local MNC-carboplatin in SRC after surgery
ng Fe/g tissue
3000
2000
1000
0
24
48
72
96
120
144
168
192
(h)

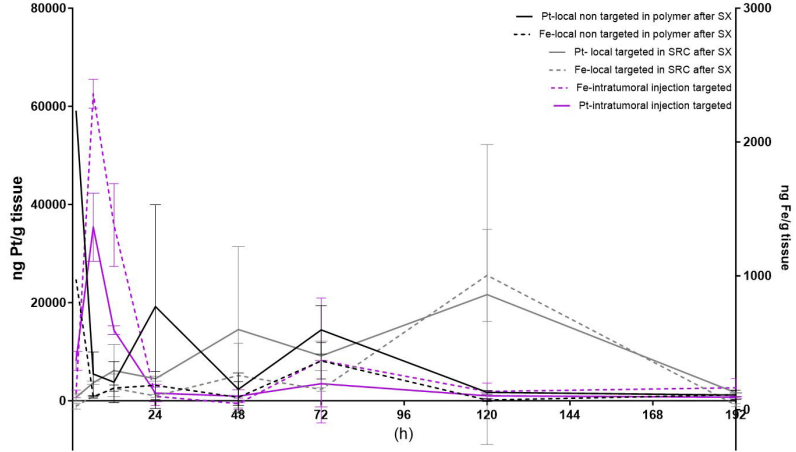
site Pt and Fe- 3 groups
Pt-local non targeted in polymer after SX
Fe-local non targeted in polymer after SX
Pt- local targeted in SRC after SX
Fe-local targeted in SRC after SX
Fe-intratumoral injection targeted
Pt-intratumoral injection targeted
ng Pt/g tissue
80000
60000
40000
20000
0
ng Fe/g tissue
3000
2000
1000
0
24
48
72
96
120
144
168
192
(h)

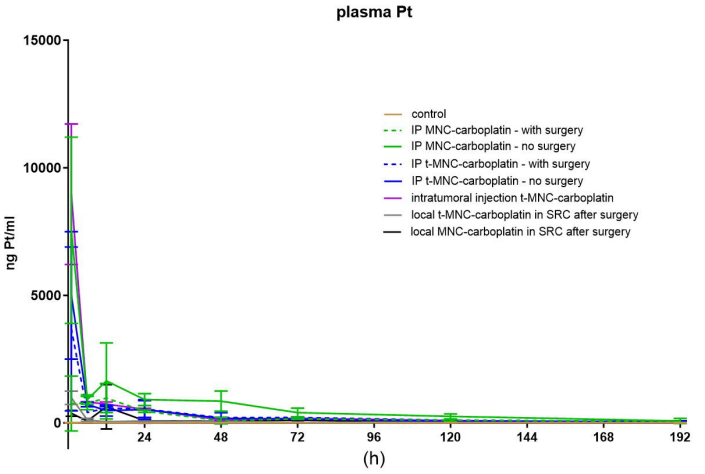
plasma Pt
ng Pt/ml
15000
10000
5000
0
24
48
72
96
120
144
168
192
(h)
control
IP MNC-carboplatin - with surgery
IP MNC-carboplatin - no surgery
IP t-MNC-carboplatin - with surgery
IP t-MNC-carboplatin - no surgery
intratumoral injection t-MNC-carboplatin
local t-MNC-carboplatin in SRC after surgery
local MNC-carboplatin in SRC after surgery

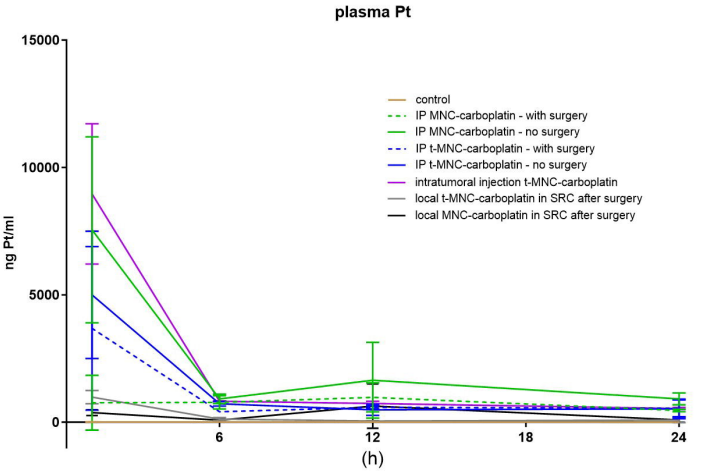
plasma Pt
ng Pt/ml
15000
10000
5000
0
6
12
18
24
(h)
control
IP MNC-carboplatin - with surgery
IP MNC-carboplatin - no surgery
IP t-MNC-carboplatin - with surgery
IP t-MNC-carboplatin - no surgery
intratumoral injection t-MNC-carboplatin
local t-MNC-carboplatin in SRC after surgery
local MNC-carboplatin in SRC after surgery

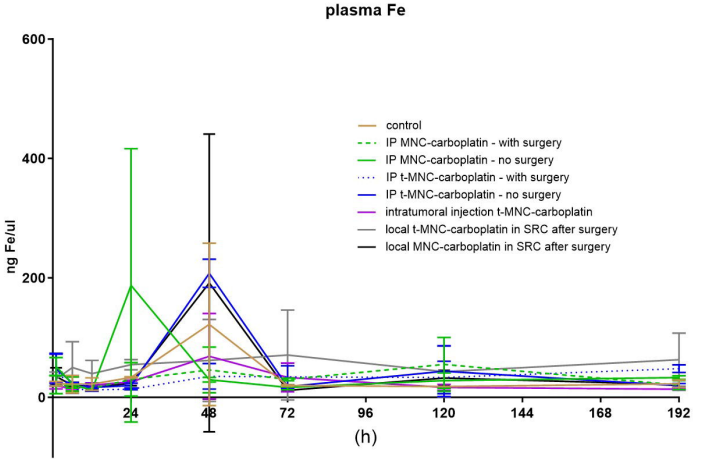
plasma Fe
ng Fe/ul
600
400
200
0
24
48
72
96
120
144
168
192
(h)
control
IP MNC-carboplatin - with surgery
IP MNC-carboplatin - no surgery
IP t-MNC-carboplatin - with surgery
IP t-MNC-carboplatin - no surgery
intratumoral injection t-MNC-carboplatin
local t-MNC-carboplatin in SRC after surgery
local MNC-carboplatin in SRC after surgery

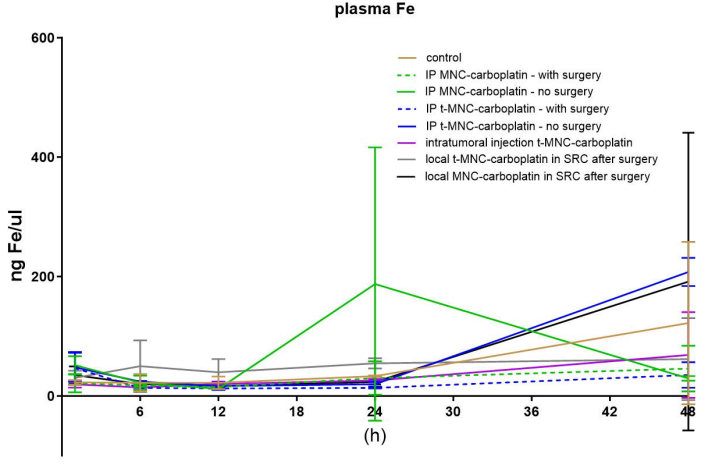
plasma Fe
ng Fe/ul
600
400
200
0
6
12
18
24
30
36
42
48
(h)
control
IP MNC-carboplatin - with surgery
IP MNC-carboplatin - no surgery
IP t-MNC-carboplatin - with surgery
IP t-MNC-carboplatin - no surgery
intratumoral injection t-MNC-carboplatin
local t-MNC-carboplatin in SRC after surgery
local MNC-carboplatin in SRC after surgery

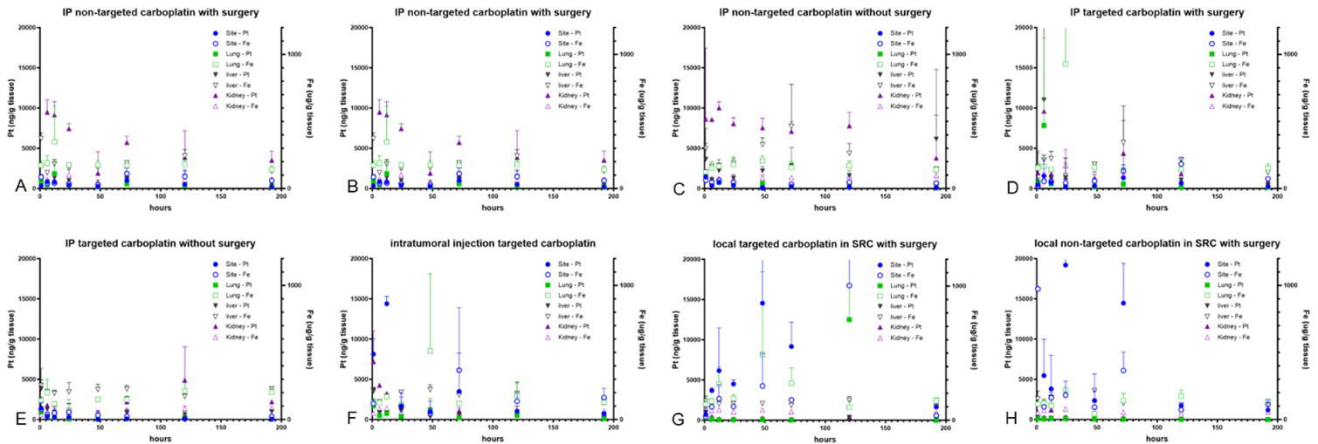
IP non-targeted carboplatin with surgery
IP non-targeted carboplatin with surgery
IP non-targeted carboplatin without surgery
IP targeted carboplatin with surgery
IP targeted carboplatin without surgery
intratumoral injection targeted carboplatin
local targeted carboplatin in SRC with surgery
local non-targeted carboplatin in SRC with surgery
Site - Pt
Site - Fe
Lung - Pt
Lung - Fe
Iver - Pt
Iver - Fe
Kidney - Pt
Kidney - Fe
Pt (ng/g tissue)
Fe (ng/g tissue)
hours
A
B
C
D
E
F
G
H